

Holocene rainfall dynamics in Central Asia

George E. A. Swann^{1,*}, Anson W. Mackay², Elena Vologina³, Matthew D. Jones¹, Virginia N. Panizzo¹,
Melanie J. Leng⁴, Hilary J. Sloane⁴, Andrea M. Snelling¹, Michael Sturm⁵

¹*School of Geography, Centre for Environmental Geochemistry, University of Nottingham, University Park,
Nottingham, NG7 2RD, UK*

²*Environmental Change Research Centre, Department of Geography, UCL, London, UK*

³*Institute of Earth's Crust, Siberian Branch of the Russian Academy of Sciences, Irkutsk, Russia*

⁴*NERC Isotope Geosciences Facilities, British Geological Survey, Nottingham, NG12 5GG, UK*

⁵*Eawag-ETH, Swiss Federal Institute of Aquatic Science and Technology, 8600, Dübendorf, Switzerland*

* *corresponding author george.swann@nottingham.ac.uk*

Keywords: Diatom; Isotope; Lake Baikal; Paleoclimatology; Precipitation

Abstract

Climate models currently provide conflicting predictions of future climate change across Central Asia. With concern over the potential for a change in water availability to impact communities and ecosystems across the region, an understanding of historical trends in precipitation is required to aid future model development and assess the vulnerability of the region to future changes in the hydroclimate. Here we present a record from Lake Baikal, located in the southern Siberian region of central Asia close to the Mongolian border, which demonstrates a clear relationship between the oxygen isotope composition of diatom silica ($\delta^{18}\text{O}_{\text{diatom}}$) and precipitation to the region over the 20th and 21st century. From this, we demonstrate that rates of precipitation in recent times are at their lowest for the past 10,000 years and identify significant long-term variations in precipitation that are not detected by current modelling efforts. With decadal changes in precipitation linked to the Atlantic Multidecadal Oscillation (AMO), our findings highlight the potential for 21st Century changes in Central Asian precipitation amidst ongoing uncertainty over the future state of the AMO and the ability of models to accurately forecast variability within it.

30 **1 Introduction**

31 The forest-steppe ecotone of Central Asia is dominated by grassland and taiga ecosystems that are vulnerable to
32 both changes in the climate and other anthropogenic activities (Craine et al., 2012; Hijjoka et al., 2014; Settele
33 et al., 2014; Tautenhahn et al., 2016). Declines in precipitation over the past three decades have led to marked
34 reductions in grassland biomass across the Mongolian steppes and wider region (Endo et al., 2006; Liu et al.,
35 2013; Li et al., 2015), whilst global reductions in boreal forest due to fire and forestry are second only to losses
36 in tropical forests (Hansen et al., 2013). Ongoing work points to the continuing fragility of these ecosystems.
37 For example, 21st Century climate change across Central Asia is likely to lead to a northward migration of the
38 forest-steppe ecotone with remaining forest stand height highly dependent on rates of precipitation
39 (Tchebakova et al., 2009; 2016). At the same time reductions in soil moisture associated with climate change
40 are expected to accelerated grassland degradation, negatively impacting nomadic pastoralism (Liu et al., 2013;
41 Sugita et al., 2015), whilst issues of water security are likely to be exacerbated by plans for increased
42 groundwater extraction and dam construction (Karthé et al., 2015). Growth of hemi-boreal forests in the forest -
43 steppe ecotone has already slowed, linked to decline soil water content due to regional warming (Wu et al.
44 2012).

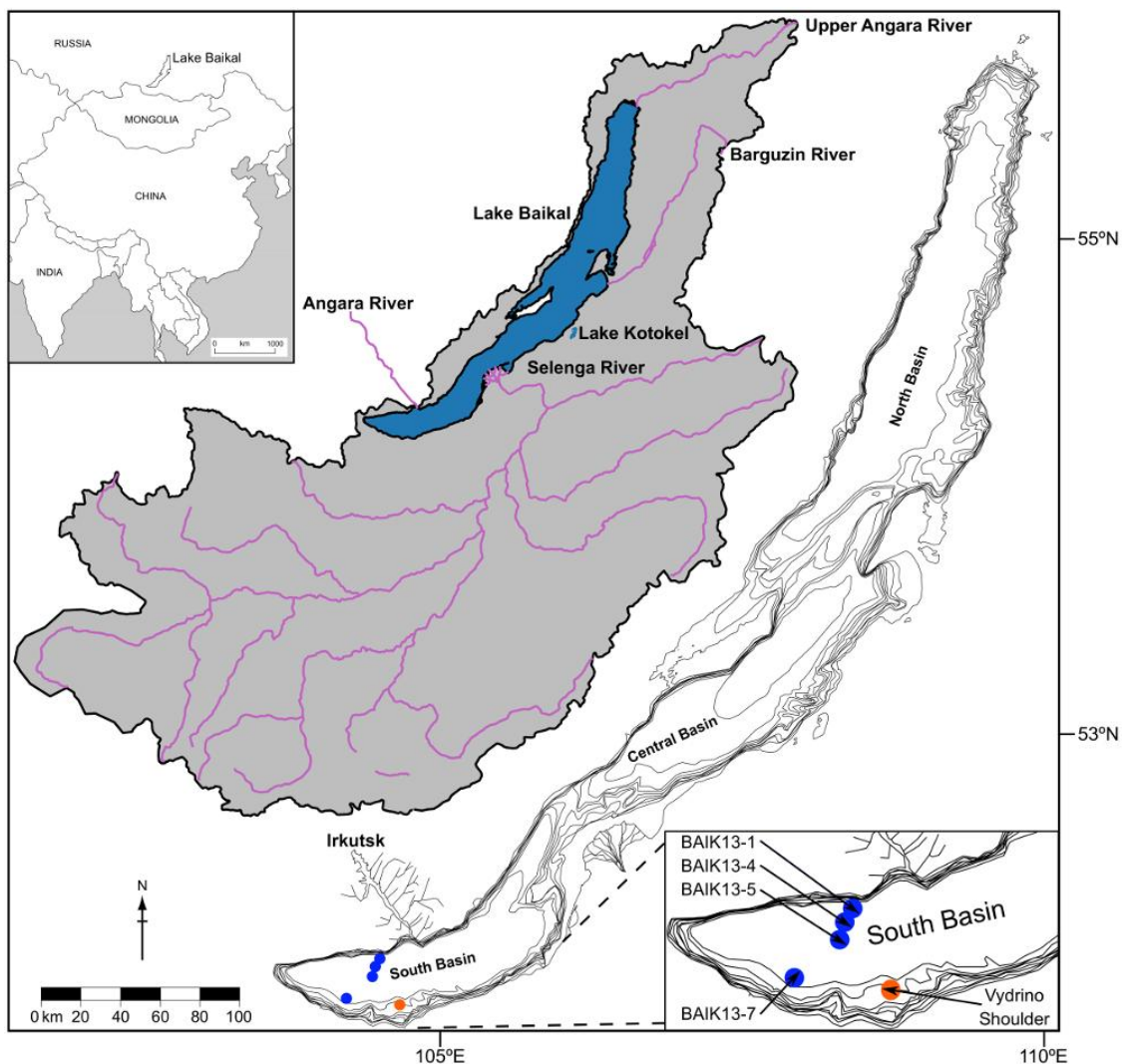
45

46 Changes in the central Asian hydrological cycle will also alter regional carbon cycling. The increased risk of
47 fires across grasslands and boreal forest will impact vegetation regeneration (Tchebakova, 2009; IPCC, 2012;
48 Tautenhahn et al., 2016) and lead to an immediate increase in atmospheric CO₂ (Randerson et al., 2006).
49 Reductions in soil moisture availability and rising temperatures will further reduce carbon terrestrial storage by
50 increasing the decomposition of organic matter in soils and lowering net carbon uptake by plants (Lu et al.,
51 2009; Crowther et al., 2016). However, more significant are the threats posed by permafrost degradation,
52 particular in southern Siberia and northern Mongolia where permafrost is vulnerable to degradation through
53 warming, human impacts and increased wildfires (Sharkuu, 1998; Romanovsky et al., 2010; Zhao et al., 2010;
54 Törnqvist et al., 2014). Combined, these processes will release carbon to the atmosphere (Schuur et al., 2015)
55 and increase organic carbon export to water bodies (Selvam et al., 2017).

56

57 In order to aid model development and so improve future predictions of the Central Asian hydrological cycle
58 there is an urgent need to understand long-term changes in the climate system beyond the instrumental record.

59 Here we use the oxygen isotope composition of diatom silica ($\delta^{18}\text{O}_{\text{diatom}}$) from Lake Baikal (Russia) to constrain
 60 historical changes in Central Asian precipitation over the last 10,000 years, within the context of the modern
 61 day. Situated at the edge of the forest-steppe ecotone, the lake's catchment extends into northern Mongolia
 62 (Fig. 1) and is highly sensitive to changes in the hydrological cycle. Future changes in the region have the
 63 potential to reduce river flow around Lake Baikal, impacting the provision of water to one of the world's
 64 greatest lakes (Törnqvist et al., 2014) as well as decreasing soil moisture content and so increasing the risk of
 65 forest fires and associated carbon release (Forkel et al., 2012). Concurrently, climate change is likely to lead to
 66 further loss of permafrost across the region (Sharkuu, 1998; Törnqvist et al., 2014), potentially increasing the
 67 flow of dissolved organic carbon into Lake Baikal (Mackay et al., 2017) and altering the microbial food web,
 68 nutrient recycling and carbon processing within this ecological sensitive lake (Moore et al., 2009).



69 Figure 1: Location of Lake Baikal and its catchment (grey region) together with Lake Kotokel, the city of
 70 Irkutsk, major rivers, coring sites BAIK13-1, BAIK13-4, BAIK13-5, BAIK13-7 (blue circles) and Vydrino
 71 Shoulder (orange circle).

72 **1.1 Lake Baikal reconstructions of the hydrological cycle**

73 Lake Baikal is the world's oldest, deepest and voluminous lake and, located in southern Siberia, contains c.
74 20% of the world's surface freshwater not stored within ice. The lake is divided into three basins (south, central
75 and north) separated by the Buguldeika Saddle and the Academician Ridge, respectively (Fig. 1). Inputs of
76 water to the lake are primarily derived from direct precipitation (16.3%) and riverine inputs (83.2%) (Seal and
77 Shanks, 1998). Groundwater inputs are minor, believed to provide <4.5% of annual inflow (Seal and Shanks,
78 1998), although no systematic study has been carried out on groundwater, its residence time or isotope
79 composition. Whilst over 350 rivers drain an area of c. 540,000 km² into Lake Baikal, inputs are dominated by
80 the Selenga River, extending south into Mongolia, and the Upper Angara and Barguzin Rivers, draining the
81 north of the catchment, which contribute c. 62%, 17% and 8% of riverine input respectively (Seal and Shanks,
82 1998) (Fig. 1).

83

84 Once in Lake Baikal, surface waters that extend down to the mesothermal maximum (MTM) at a depth of 200-
85 300 m undergo convective mixing (Shimaraev et al., 1994; Shimaraev and Domysheva, 2004) and wind forced
86 convection (Troitskaya et al., 2015). Whilst deeper waters are stratified (Shimaraev and Granin, 1991;
87 Shimaraev et al., 1994; Ravens et al., 2000), they are exchanged across the MTM through periodic upwelling
88 and downwelling episodes (Weiss et al., 1991; Shimaraev et al., 1993, 1994, 2012; Kipfer et al., 1996;
89 Hohmann et al., 1997). Finally, water loss from Lake Baikal is dominated by outflow through the Angara River
90 in the south basin of Lake Baikal (c. 81%) and evaporation (c. 19%), with an additional unconstrained loss
91 from groundwater estimated at <2% of total outflow (Seal and Shanks, 1998; Shimaraev et al., 1994).

92

93 Over the past 15 years, significant effort has been devoted towards developing and applying $\delta^{18}\text{O}_{\text{diatom}}$ in
94 palaeoenvironmental reconstructions due to its ability to reflect the isotope composition of ambient water
95 ($\delta^{18}\text{O}_{\text{water}}$). With the controls on $\delta^{18}\text{O}_{\text{diatom}}$ similar to those for carbonates, $\delta^{18}\text{O}_{\text{diatom}}$ represents an important source
96 of information in aquatic ecosystems such as Lake Baikal where carbonates are poorly preserved (Leng and
97 Barker, 2006). In Lake Baikal, mixing of the water column leads to uniform surface and deep $\delta^{18}\text{O}_{\text{water}}$ of -15.8
98 $\pm 0.2\text{‰}$, whilst riverine inputs ($\delta^{18}\text{O}_{\text{river}}$) vary latitudinally in relation to the isotopically low winter precipitation
99 in the north ($\delta^{18}\text{O}_{\text{p}}$) and higher summer $\delta^{18}\text{O}_{\text{p}}$ in the south (Seal and Shanks, 1998; Morley et al., 2005). With
100 riverine inputs accounting for >80% of all inflow to the lake, spatial and temporal changes in $\delta^{18}\text{O}_{\text{p}}$ across the

101 catchment have been proposed to change both $\delta^{18}\text{O}_{\text{river}}$ and the relative balance of north versus south basin river
102 discharge to the lake, processes that in turn alter $\delta^{18}\text{O}_{\text{water}}$ (Morley et al., 2005). On this basis, records of
103 $\delta^{18}\text{O}_{\text{diatom}}$ can be used to monitor changes in the regional Central Asian hydroclimate.

104

105 To date, this interpretation has been applied to interglacial records from Lake Baikal spanning the Holocene,
106 MIS 5e and MIS 11 to constrain temporal variations in the penetration of westerlies into Central Asia and
107 regional atmospheric circulation involving the Siberian High (Mackay et al., 2008, 2011, 2013). However, no
108 empirical relationship has been demonstrated between hydroclimate variability and down-core records of
109 $\delta^{18}\text{O}_{\text{diatom}}$. The absence of such a calibration prevents: 1) a full quantitative interpretation of the $\delta^{18}\text{O}_{\text{diatom}}$ data
110 from Lake Baikal; 2) the integration of hydroclimate information in data-model comparisons to validate climate
111 model outputs and direct climate model development (e.g., Haywood et al., 2016); and 3) insight of how the
112 regional Central Asian climate behaved in intervals which might represent a future climate state. Here we
113 consider point #1 through the presentation of new $\delta^{18}\text{O}_{\text{diatom}}$ data from a series of cores from the south basin of
114 Lake Baikal that are compared to metrological data over the last century and then employed to constrain
115 historical changes in Central Asian precipitation through the Holocene. In demonstrating a relationship between
116 $\delta^{18}\text{O}_{\text{diatom}}$ and precipitation, we highlight that levels of precipitation are today at their lowest levels for the last
117 10,000 years (10 ka), indicating the vulnerability of the region to future changes in precipitation and its
118 associated impact on ecosystem disturbance and terrestrial carbon cycling.

119

120 **2 Method**

121 **2.1 Sediment coring**

122 Four short sediment cores were collected from the south basin of Lake Baikal in March and August 2013 using
123 a UWITEC corer with PVC-liners ($\text{\O} 63 \text{ mm}$) which provided complete and undisturbed recovery of the highly
124 susceptible sediment/water interface of the cores (Fig. 1). Multiple cores were collected from each of the sites
125 in March 2013 through c. 78–90 cm of ice: BAIK13-1 ($51^{\circ}46'04.2''\text{N}$, $104^{\circ}24'58.6''\text{E}$, water depth = 1,360 m),
126 BAIK13-4 ($51^{\circ}41'33.8''\text{N}$, $104^{\circ}18'00.1''\text{E}$, water depth = 1,360 m) and BAIK13-5 ($51^{\circ}39'01.9''\text{N}$,
127 $104^{\circ}16'26.8''\text{E}$, water depth = 1,350 m). Further cores were then collected from BAIK13-7 ($51^{\circ}34'06''\text{N}$,
128 $104^{\circ}31'43''\text{E}$, water depth = 1,080 m) in August 2013 aboard the Geolog research boat from the Institute of the
129 Earth's Crust/Irkutsk (Fig. 1). At each site one core (BAIK13-1C [50 cm], BAIK13-4F [33 cm], BAIK13-5C

130 [42 cm], BAIK13-7A [47.5 cm]) was sub-sampled in the field at a resolution of 0.2 cm and transported to the
131 UK for $\delta^{18}\text{O}_{\text{diatom}}$ analysis. Parallel cores (BAIK13-1A [49.3 cm], BAIK13-4C [38.3 cm], BAIK13-5A [43.4
132 cm], BAIK13-7B [47.2 cm]) were transferred to the Institute of the Earth's Crust/Irkutsk before being cut,
133 photographed and lithologically described, based on smear slide inspection. A Bartington MS2E High
134 Resolution Surface Scanning Sensor (Bartington, 1995) was used for non-destructive measurement of magnetic
135 susceptibility (MS), with a resolution of 1 cm.

136

137 **2.2 Age models**

138 Dried samples from BAIK13-1C, BAIK13-4F and BAIK13-7A were analysed for ^{210}Pb , ^{226}Ra , ^{137}Cs and ^{241}Am
139 by direct gamma assay in the Environmental Radiometric Facility at University College London, using ORTEC
140 HPGe GWL series well-type coaxial low background intrinsic germanium detector. No dating was carried out
141 on core BAIK13-5C. Instead, results from BAIK13-5C are included for the purpose of qualitative comparisons
142 with $\delta^{18}\text{O}_{\text{diatom}}$ data from other sites. ^{210}Pb was determined via its gamma emissions at 46.5keV and ^{226}Ra by
143 emissions of its daughter isotope ^{214}Pb at 295keV and 352keV following storage for three weeks in sealed
144 containers to allow radioactive equilibration. ^{137}Cs and ^{241}Am were measured by their emissions at 662keV and
145 59.5keV (Appleby et al, 1986). Corrections were made for the effect of self-absorption of low energy gamma
146 rays within the sample (Appleby et al, 1992), with the absolute efficiencies of the detector determined using
147 calibrated sources and sediment samples of known activity. To construct the final age-depth models a
148 polynomial regression was fitted to the ^{210}Pb data with additional degrees added until no further improvements
149 occurred at the 95% confidence interval.

150

151 **2.3 Diatom oxygen isotopes**

152 Thirty samples from cores BAIK13-1C, BAIK13-4F, BAIK13-5C, BAIK13-7A were prepared for diatom
153 isotope analysis (see Supplementary Table 1) using a combination of reagents to remove contaminants and
154 heavy liquid separation (Swann et al., 2013). Prior to analyses all samples were screened using a Zeiss Axiovert
155 40 C inverted microscope, scanning electron microscope (SEM) and X-ray fluorescence (XRF) to confirm
156 sample purity and the absence of non-diatom contaminants. Diatoms in the analysed samples are dominated by
157 mainly endemic species including *Aulacoseira baicalensis*, *Aulacoseira skvortzowii*, *Crateriportula*
158 *inconspicua*, *Cyclotella minuta*, *Stephanodiscus meyerii* and *Synedra acus* var. *radians*. Given the functional

159 ecology of taxa in the analysed samples, our isotope records are interpreted as recording mean annual
160 conditions with a significant bias towards spring months when diatom productivity peaks shortly after ice
161 break-up (Popovskaya, 2000).

162

163 Samples were analyzed for $\delta^{18}\text{O}_{\text{diatom}}$ using a step-wise fluorination procedure at the NERC Isotope Geosciences
164 Facility based at the British Geological Survey (Leng and Sloane, 2008). Isotope measurements were made on a
165 Finnigan MAT 253 and converted to the Vienna Standard Mean Ocean Water (VSMOW) scale using the
166 within-run laboratory diatom standard BFC_{mod} calibrated against NBS28. Where necessary, samples were
167 corrected for oxygen bearing contaminants using a geochemical mass balance approach developed for Lake
168 Baikal (Mackay et al., 2011). The issue of contaminants can be problematic in Lake Baikal due to
169 aluminosilicates trapped within the cylindrical frustules of *Aulacoseira* species (Brewer et al., 2008). To
170 account for this, contaminants were calculated using XRF Al_2O_3 concentrations, corrected for an assumed
171 diatom bound Al concentration of 0.3 wt%, and used to model contaminant oxygen using Lake Baikal end-
172 members in which aluminosilicates contain 17.2% Al with a $\delta^{18}\text{O}$ composition of 11.7‰ (Brewer et al., 2008;
173 Mackay et al., 2011).

174

175 **2.4 Climatological data**

176 To assess the controls on $\delta^{18}\text{O}_{\text{diatom}}$, results were compared to climatological data from World Meteorological
177 Organisation station 30710 (52°16'20" N, 104°18'29" E, elevation = 467 m), located in Irkutsk close to the south
178 basin of Lake Baikal (Fig. 1) with data from 2016-1891 obtained via the KNMI Climate Explorer
179 (<http://climexp.knmi.nl/>). Values of $\delta^{18}\text{O}_p$ were calculated following Seal and Shanks (1998) who established a
180 relationship ($r^2 = 0.768$) between $\delta^{18}\text{O}_p$ and surface air temperature (SAT) of:

181

$$182 \quad \delta^{18}\text{O}_p = 0.361 \cdot \text{SAT} - 16.798$$

183

(Eq. 1)

184 With >95.5% of water inputs to the lake originating from direct precipitation or riverine inputs (Seal and
185 Shanks, 1998), changes in monthly isotopic inputs to Lake Baikal can be obtained by multiplying $\delta^{18}\text{O}_p$ by the
186 amount of monthly precipitation to account for seasonal variations in precipitation. Monthly values can then be
187 summed to calculate annual inputs with values normalised relative to results for 2016 (δ_{influx}):

$$\delta_{\text{influx}} = \left(\frac{\sum_{\text{January}}^{\text{December}} \delta^{18}\text{O}_p \cdot \text{Precipitation (mm/month}^{-1})}{\text{Days in year}} \right) / \delta_{2016\text{influx}}$$

188 (Eq. 2)

189

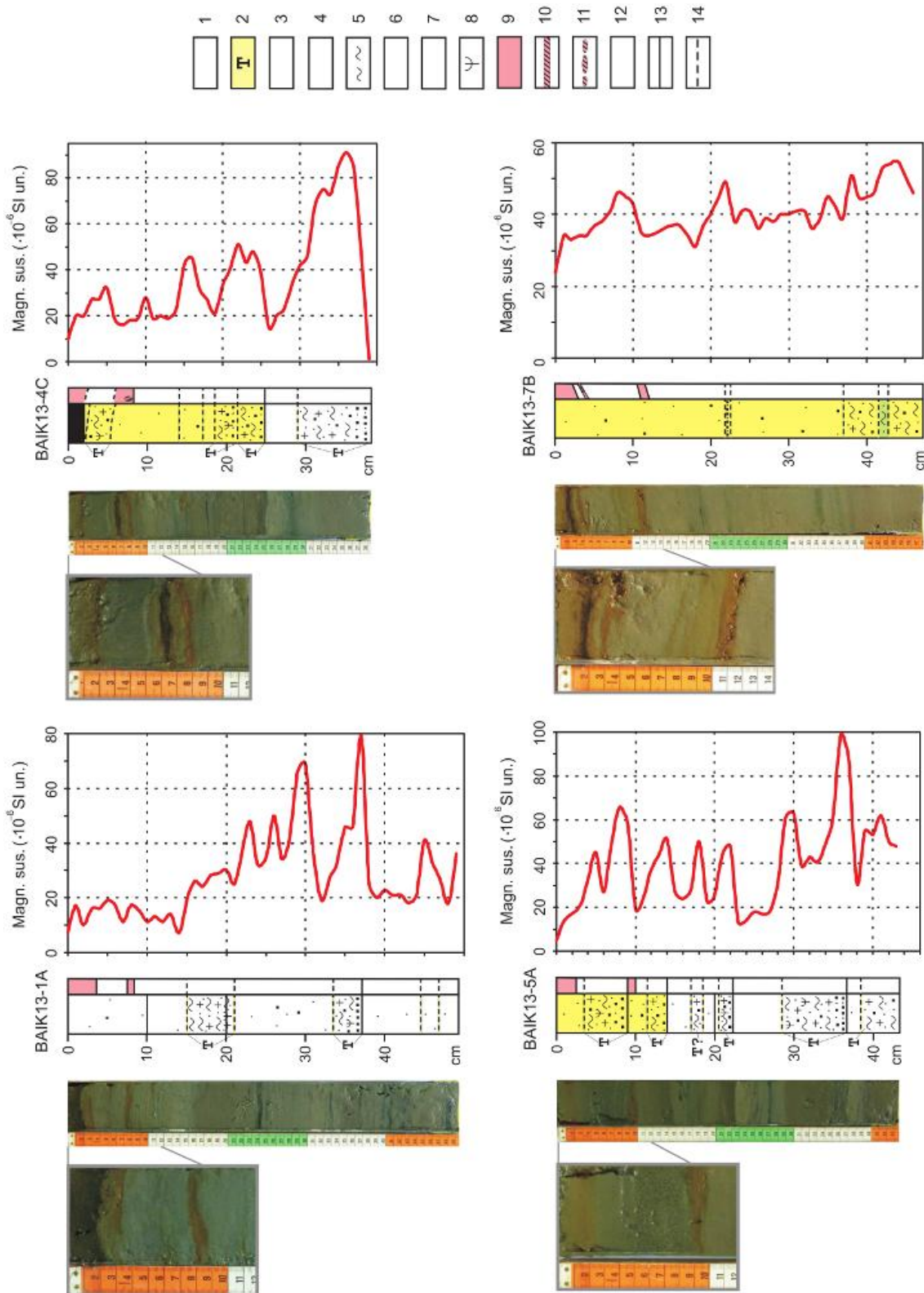
190 **3 Results**

191 **3.1 Core lithology**

192 The deep water sediments of Lake Baikal are characterized by homogenous, fine-grained, and grey to olive-
 193 grey pelagic muds. They primarily consist of autochthonous biogenic material (mainly diatoms) with small
 194 amounts of allochthonous, terrigenous material (including pollen grains, clayey silts and a few sand grains).
 195 The entire water column of Lake Baikal is saturated throughout with oxygen, due to the regular renewal of the
 196 deep waters (Shimaraev et al., 1994; Tsimitri et al., 2015), which results in the oxidation of even the deepest
 197 surface sediment. Cores BAIK13-1A, BAIK13-4C, BAIK13-5A and BAIK13-7B are oxidized down to a depth
 198 of 2.0-3.6 cm, showing olive-brown, dark-brown to brownish-black colours (Fig. 2). Core BAIK13-7B
 199 recovered closer to the southern shore of the south basin consists of slightly more coarse-grained sediments
 200 with an increased content of silt and sand (Fig. 2). The homogenous pelagic muds of the deep-water basins of
 201 the lake are frequently intercalated by coarse turbidite layers. These graded beds are characterized by
 202 allochthonous, mostly terrigenous material, higher magnetic susceptibility and a graded texture, which grades
 203 upwards from a sandy base to silty-pelitic deposits with few sand admixtures and occasionally overlain at the
 204 top by a thin pelitic mud layer (Vologina et al., 2007; Sturm et al., 2016).

205

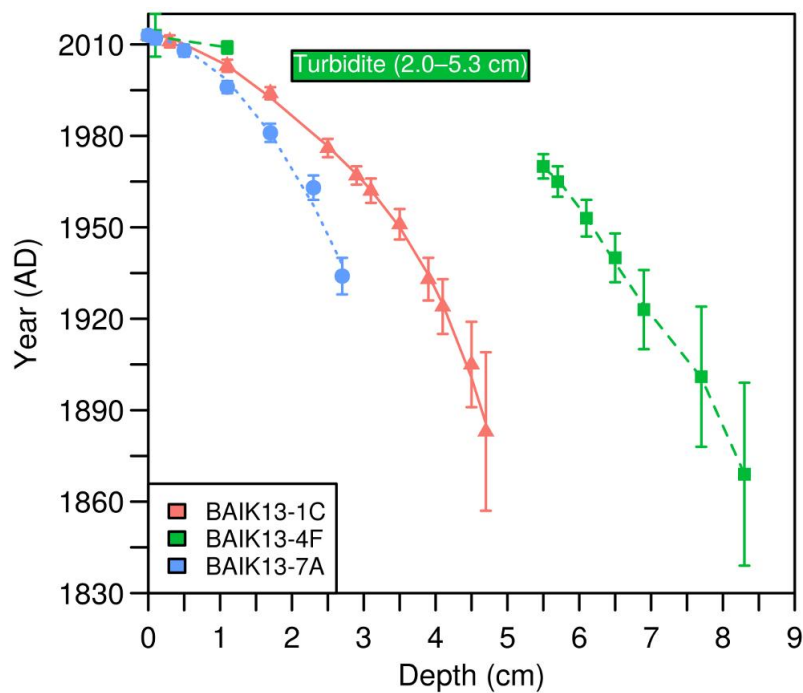
206 Several turbidites at different core depths and various thicknesses between 1.8 cm and 9.0 cm were observed in
 207 the cores, with two turbidites in BAIK13-1A, three in BAIK13-4C and six in BAIK13-5A (Fig. 2). The
 208 uppermost turbidites occur at 15.0–21.0 cm (BAIK13-1A), 2.0–5.3 cm (BAIK13-4C) and 3.5–9.0 cm
 209 (BAIK13-5A). There are layers of sand (21.8–22.5 cm) and sandy sediments (37.0–41.5 cm, 42.5–47.2 cm)
 210 without graded texture within sediment core BAIK13-7B. Lithological descriptions and MS-results were used
 211 to aid sampling of pelagic biogenic sediments (MS-values of up to 30×10^{-6} SI units) and avoid both turbidites
 212 and sandy layers (MS-values of up to 99×10^{-6} SI units).



213 Figure 2: Photos, lithology and magnetic susceptibility of sediment cores BAIK13-1A, BAIK13-4C, BAIK13-
 214 5A and BAIK13-7B from the south basin of Lake Baikal. Lithology (left column): 1 - pelagic mud, 2 -
 215 turbidite, 3 - sandy sediment, 4 - diatoms, 5 - clay, 6 - silt, 7 - sand, 8 - land plant remains. Right column: 9 -
 216 oxidized sediment, 10 - Fe/Mn crust, 11 - fragments of Fe/Mn crust, 12 – O₂ reduced sediment. Boundaries
 217 between layers: 13 - distinct boundaries between layers, 14 - indistinct boundaries between layers.

218 3.2 ²¹⁰Pb age models

219 Total ²¹⁰Pb activity reaches equilibrium with supported ²¹⁰Pb at a depth of c. 5 cm (BAIK13-1C), 9 cm
220 (BAIK13-4F) and 4 cm (BAIK13-7A). At sites BAIK13-1C and BAIK13-4F well resolved peaks of ¹³⁷Cs at 3.1
221 cm and 5.5-5.7 cm respectively likely relate to peak atmospheric testing of nuclear weapons 1963 AD. At all
222 sites, non-monotonic variation in unsupported ²¹⁰Pb prevented the use of the constant initial concentration (CIC)
223 dating model. Instead, ²¹⁰Pb dates were calculated using the constant rate of ²¹⁰Pb supply (CRS) model
224 (Appleby and Oldfield, 1978). At BAIK13-1C and BAK13-4F depths of 3.1 cm and 5.7 cm are dated to
225 1962/1963 AD respectively, both in agreement with the ¹³⁷Cs record. An absence of clear peaks in either ¹³⁷Cs
226 or ²⁴¹Am at BAIK13-7A prevents validation of the ²¹⁰Pb dates. For all sites the final age-depth model shows a
227 good fit to the ²¹⁰Pb dates (BAIK13-1C Adjusted R² > 0.99; BAIK13-4F Adjusted R² = > 0.99; BAK13-7A
228 Adjusted R² > 0.99) (Fig. 3). Mean uncertainty in the individual ²¹⁰Pb dates across all three cores is 6.8 years
229 (BAIK13-1C: \bar{x} = 7, range = 2-26; BAIK13-4F: \bar{x} = 8, range = 2-30; BAIK13-7A: \bar{x} = 3, range = 2-6) (Fig. 3).



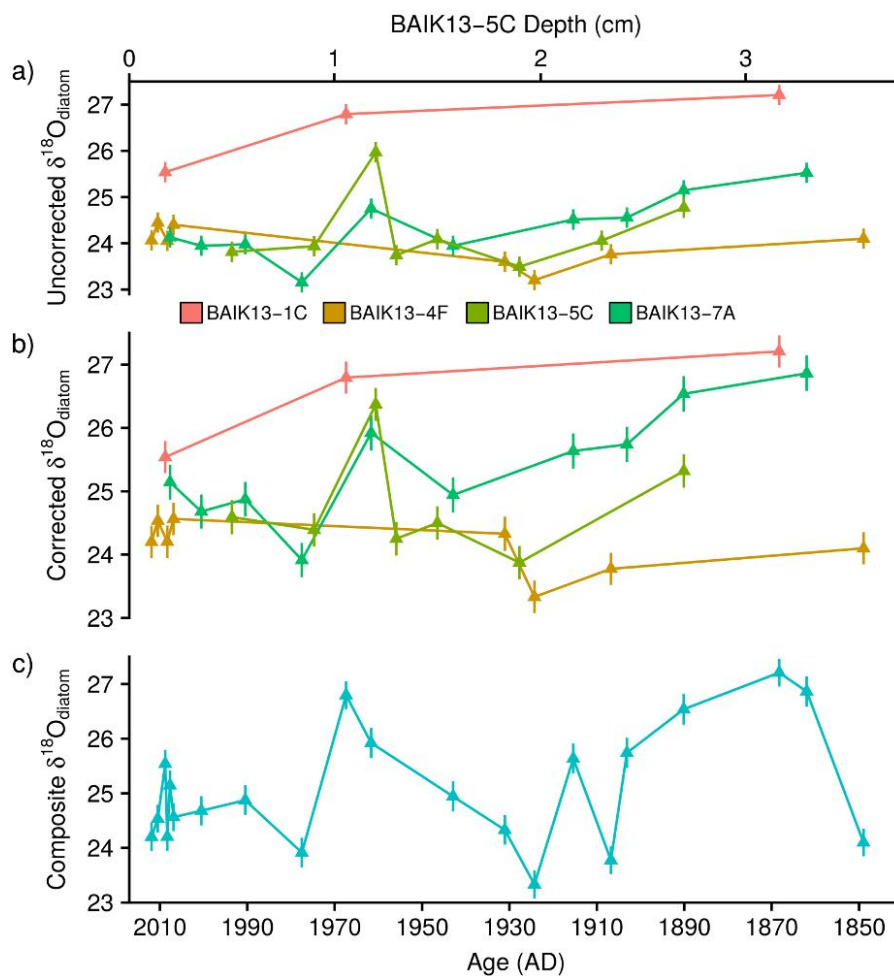
230 Figure 3: ²¹⁰Pb age-depth models for cores BAIK13-1C, BAIK13-4F and BAIK13-7A.

231

232 3.3 $\delta^{18}\text{O}_{\text{diatom}}$

233 Analysed samples from the four sediment cores cover the interval from c. 2010-1850 AD with raw $\delta^{18}\text{O}_{\text{diatom}}$
234 varying from +23.2‰ to +28.1‰ and replicate analyses of sample material indicating an analytical
235 reproducibility (1 σ) of 0.2‰ (Fig. 4a). Results from BAIK13-5C, which does not have an age model, display

236 similar values and variations to those in BAIK13-4F and BAIK13-7C, although values at BAIK13-1C are
 237 notably higher at +25.5‰ to +27.2‰. Levels of contamination were minimal for cores BAIK13-1C (\bar{x} = 0%
 238 contamination), BAIK13-4F (\bar{x} = 1.7% contamination) and BAIK13-5C (\bar{x} = 3.9% contamination) with Al/Si
 239 ratios of <0.02. At BAIK13-7C Si/Al ratios increase to 0.018-0.027 (\bar{x} = 0.023) indicating the need to account
 240 for aluminosilicates. Following correction for contaminants on samples at all sites, $\delta^{18}\text{O}_{\text{diatom}}$ ranges from
 241 +23.3‰ to +27.2‰ (\bar{x} = +24.5‰, 1σ = 1.0‰) (Fig. 4b) with the propagation of error associated with the
 242 correction increasing the analytical uncertainty for individual samples to 0.25-0.28‰. The two samples without
 243 XRF data are not considered further in this manuscript and all further mention of $\delta^{18}\text{O}_{\text{diatom}}$ refers to the
 244 corrected $\delta^{18}\text{O}_{\text{diatom}}$ dataset (Supplementary Table 1).



245 Figure 4: $\delta^{18}\text{O}_{\text{diatom}}$ from the south basin of Lake Baikal. Raw (uncorrected) (A) and corrected (B) $\delta^{18}\text{O}_{\text{diatom}}$
 246 together with the composite south basin $\delta^{18}\text{O}_{\text{diatom}}$ record (C). All samples plotted against age except for
 247 BAIK13-5C, which are plotted against depth and not used in the final composite $\delta^{18}\text{O}_{\text{diatom}}$ record. Error bars for
 248 uncorrected $\delta^{18}\text{O}_{\text{diatom}}$ data are the 1σ analytical reproducibility (0.2‰) with error bars for the corrected $\delta^{18}\text{O}_{\text{diatom}}$
 249 data reflecting the propagation of error associated with the correction for contaminants (range = 0.25-0.28‰).

250

251 On the basis of homogeneity in $\delta^{18}\text{O}_{\text{water}}$ across the modern lake and through the water column (Seal and
252 Shanks, 1998; Morley et al., 2005), $\delta^{18}\text{O}_{\text{diatom}}$ data from sites BAIK13-1C, BAIK13-4F and BAIK13-7C are
253 combined to create a composite record of south basin $\delta^{18}\text{O}_{\text{diatom}}$ ranging from +23.3‰ to +27.2‰ (\bar{x} = +25.1‰,
254 1σ = 1.1) (Fig. 4c). After c. 1850 (+24.1‰), $\delta^{18}\text{O}_{\text{diatom}}$ increases in the second half of the 19th century to higher
255 values of +25.1‰ to +27.2‰. Through the 20th century $\delta^{18}\text{O}_{\text{diatom}}$ is variable (\bar{x} = +24.2‰, 1σ = 1.1‰),
256 particularly from 1960-1970 when $\delta^{18}\text{O}_{\text{diatom}}$ reaches a minimum of +23.2‰ by the end of the 1970's and a peak
257 of +26.8‰ in the late 1960's. Values of $\delta^{18}\text{O}_{\text{diatom}}$ in the decade before the cores were collected in 2013 vary
258 from +24.1‰ to +25.5‰ (\bar{x} = +24.5‰, 1σ = 0.6‰).

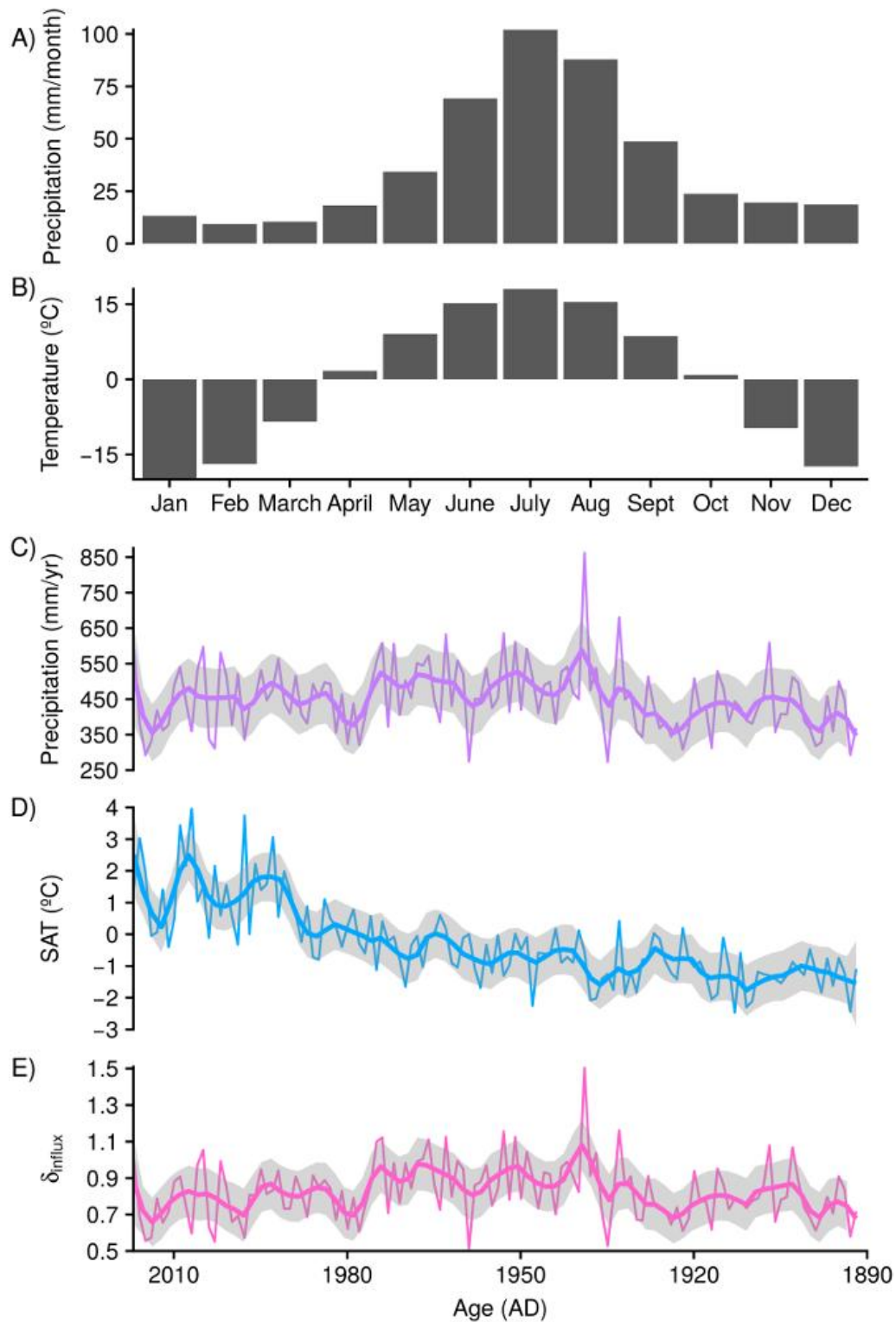
259

260 **3.4 δ_{influx}**

261 Mean annual precipitation in Irkutsk is 450 mm/yr with c. 75% of precipitation falling in the extended summer
262 period from May to September, and only <10% falling in winter (DJF) (Fig. 5a). Surface air temperatures show
263 similar seasonal variations from -20°C in January to +18°C in July (Fig. 5b). No systematic change in
264 precipitation is apparent for recent decades, although precipitation from 2016-1926 (\bar{x} = 466 mm/yr) is notably
265 higher than 1925-1891 (\bar{x} = 410 mm/yr, $p < 0.001$) after the step change in 1926 (Fig. 5c). In line with global
266 records, SAT at Irkutsk show a prolonged warming trend over the monitoring record with marked increases
267 from c. 1950 and c. 1990 onwards that are predominantly associated with increases in winter SAT (Fig. 5d).
268 Annual and seasonal trends in precipitation and SAT from Irkutsk are similar to data from other sites around
269 Lake Baikal, with similar trends observed in records of water inflow to the lake (Shimaraev et al., 2002;
270 Frolova et al., 2017). As such, the meteorological data from Irkutsk can be regarded as being representative of
271 the wider region.

272

273 Values of δ_{influx} shows mean inter-annual variations of c. 0.17 from 2016-1891 (Fig. 5e). On decadal timescales,
274 from 1923-1891 δ_{influx} varies by c. 0.58 (\bar{x} = 0.79‰, 1σ = 0.13) before a long-term increase to the maxima in
275 1938 of 1.50, caused by exceptionally high June 1938 rainfall of 318 mm. Thereafter, values reveal a long-term
276 decline from mean 1970-1950 values of c. 0.9 to mean values of 0.77 since the year 2000.



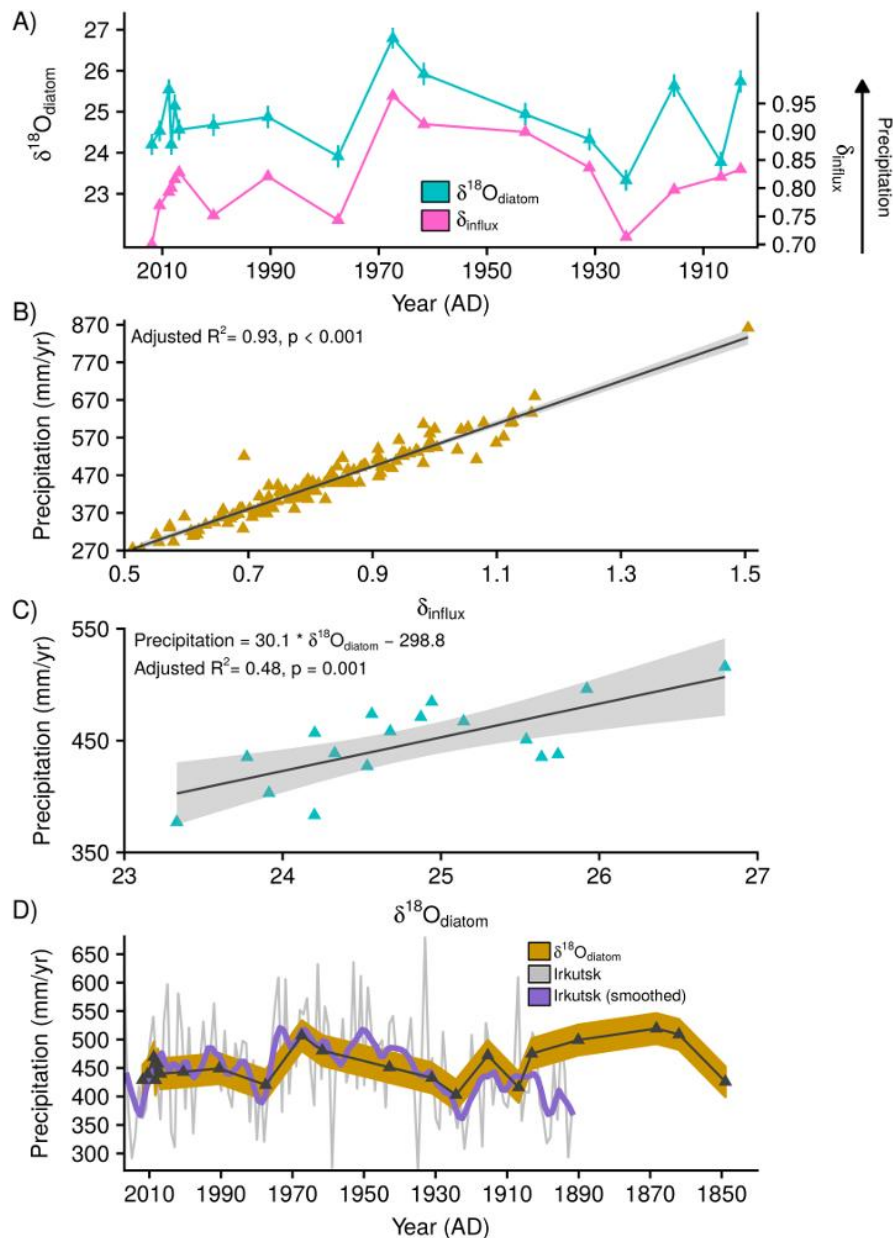
277 Figure 5: Metrological data from Irkutsk (World Meteorological Organisation station 30710) showing the (A)
 278 monthly distribution of precipitation and (B) surface air temperature (SAT) alongside (C) temporal changes in
 279 precipitation and (D) surface air temperature from 2016-1891. Values of δ_{influx} (E) are calculated following
 280 Equations 1 and 2 with all values normalised relative to a value of 1 for 2016 AD. Thicker lines for panels C-E
 281 show locally weighted smoothing (loess) with shaded regions representing the 95% confidence interval on the
 282 fitted values.

283 **3.5 Comparison of $\delta^{18}\text{O}_{\text{diatom}}$ and δ_{influx}**

284 To account for uncertainty in the age-model and with analysed samples containing diatoms that accumulated
285 over multiple years, a locally-weighted polynomial regression (lowess) was applied to δ_{influx} with a span of 10
286 years in order to enable robust comparisons with $\delta^{18}\text{O}_{\text{diatom}}$. From c. 2010-1900 change in $\delta^{18}\text{O}_{\text{diatom}}$ are
287 significantly correlated to δ_{influx} ($r = 0.72$ $p = 0.001$) with a linear regression revealing a significant relationship
288 between the two variables (Adjusted $R^2 = 0.48$, $p = 0.001$) (Fig. 6a). Whilst the residence time of water in the
289 south basin is closer to 80-90 years (Shimaraev et al., 1994), the age of surface waters down to the mesothermal
290 maximum (200–300 m water depth) are likely to be less, given reduced rates of mixing with deep/bottom
291 waters (Weiss et al., 1991). The duration of vertical exchanges across the lake is limited to a short timeframe
292 each year, with rates varying spatially across individual basins and between coastal and non-coastal sites
293 (Weiss et al., 1991; Shimaraev et al., 1994; Ravens et al., 2000; Shimaraev et al., 2012; Troitskaya et al., 2015).
294 With the mechanisms and extent of vertical mixing across Lake Baikal therefore remaining relatively
295 unconstrained, it becomes impossible to accurately model the age of the ambient water in which the analysed
296 diatoms photosynthesised. The span of 10 year employed in the regression of δ_{influx} is considered to be an
297 appropriate estimate for this, given that surface $\delta^{18}\text{O}_{\text{water}}$ is likely to be significantly weighted towards more
298 recent inputs to the lake.

299

300 Variance partitioning of δ_{influx} against surface air temperature and precipitation data from Irkutsk reveals 94% of
301 the variability in δ_{influx} is related to changes in precipitation. This is confirmed by the significant linear
302 relationship between δ_{influx} and annual precipitation at Irkutsk from 2016-1891 AD (Adjusted $R^2 = 0.93$, $p <$
303 0.001) and hence between decadal smoothed annual precipitation (span = 10 years) and $\delta^{18}\text{O}_{\text{diatom}}$ (Adjusted $R^2 =$
304 0.48 , $p = 0.001$, SE = 26.9 mm/yr) (Fig. 6 b,c). From this relationship, quantitative reconstructions of decadal
305 averaged annual precipitation can be made from $\delta^{18}\text{O}_{\text{diatom}}$ with results, when applied to the south basin
306 composite record, ranging from c. 400-520 mm/yr with variations between samples of up to 80 mm (Fig. 6d).
307 These reconstructed estimates of precipitation are offset from actual measured levels of precipitation at Irkutsk
308 by 5-45 mm/yr ($\bar{x} = 22.6$ mm/yr) (Fig. 6d).



309 Figure 6: A) Composite $\delta^{18}\text{O}_{\text{diatom}}$ and δ_{influx} from c. 2010-1900 AD showing the strong correlation ($r = 0.72$ $p =$
 310 0.001) and linear relationship (Adjusted $R^2 = 0.48$, $p = 0.001$) between the two variables. Displayed values of
 311 δ_{influx} are obtained from a locally weighted smoothing (span = 10 years) of the raw δ_{influx} data to account for
 312 uncertainty in the ^{210}Pb age model and accumulation of diatoms in the sediment record over multiple years. B)
 313 Linear relationship between raw δ_{influx} and Irkutsk annual precipitation from 2016-1891. C) Linear relationship
 314 between $\delta^{18}\text{O}_{\text{diatom}}$ and locally weighted Irkutsk precipitation (span = 10 years). D) Decadal annual precipitation
 315 reconstructed from $\delta^{18}\text{O}_{\text{diatom}}$ (brown region/black line) together with Irkutsk annual precipitation (grey) and
 316 locally weighted (span = 10 years) Irkutsk precipitation (purple). Shaded region for reconstructed precipitation
 317 is the standard error (26.9 mm/yr) of the regression model between $\delta^{18}\text{O}_{\text{diatom}}$ and Irkutsk precipitation (Fig. 6c).
 318 For clarity the y-axis has been scaled to not show the extreme Irkutsk precipitation of 861.9 mm^{-1} in 1938 AD.

319 **4 Discussion**

320 **4.1 $\delta^{18}\text{O}_{\text{diatom}}$ as an indicator of Central Asian precipitation**

321 Both $\delta^{18}\text{O}_p$ and $\delta^{18}\text{O}_{\text{river}}$ in the Lake Baikal catchment fall on or close to the global meteoric water line (Seal and
322 Shanks, 1998) with evaporation believed to not significantly impact $\delta^{18}\text{O}_{\text{water}}$ (Morley et al., 2005). With
323 changes in the amount of precipitation dominating variations in δ_{influx} (Fig. 6b), δ_{influx} can be interpreted as
324 primarily reflecting decadal changes in annual precipitation and in particular summer precipitation which
325 accounts for 70-90% of annual precipitation to the region (Fig. 5b; Afanasjev, 1976; Shimaraev et al., 1994).
326 As $\delta^{18}\text{O}_{\text{diatom}}$ reflects the isotope composition of ambient water in Lake Baikal, sedimentary records of $\delta^{18}\text{O}_{\text{diatom}}$
327 should also reflect changes in regional Central Asian precipitation. This is supported by the strong correlation
328 and relationship between δ_{influx} and $\delta^{18}\text{O}_{\text{diatom}}$, with increases (decrease) in $\delta^{18}\text{O}_{\text{diatom}}$ associated with higher
329 (lower) δ_{influx} and an increase (decrease) in precipitation (Fig. 6a), as well as by the linear relationship between
330 $\delta^{18}\text{O}_{\text{diatom}}$ and decadal smoothed annual precipitation (Fig. 6c).

331

332 The continental interior location of Lake Baikal results in intra-annual variations in precipitation being a
333 function of summer westerlies and the winter Siberian High (Lydolph, 1977). In spring the intensification of
334 zonal circulation leads to the westerly progression of cyclones to the region, a process that intensifies in
335 summer as low-pressure systems continue to develop along the Asiatic polar front (Lydolph, 1977; Chen et al.,
336 1991; Shahgedanova 2002). With summer precipitation and inter-annual variations within it closely linked to
337 eastward-propagating Rossby waves along the Asian Polar Front Jet (Iwao and Ttakahashi 2006, 2008),
338 variations in summer Siberian precipitation have been linked to the Atlantic Multidecadal Oscillation (AMO)
339 (Sun et al., 2015). Related to sea surface temperatures (SST) in the North Atlantic Ocean, the warm SST
340 associated with a positive phase of the AMO are proposed to enhance precipitation across Siberia through a
341 northerly shift in Rossby waves. Records of $\delta^{18}\text{O}_{\text{diatom}}$ from Lake Baikal can therefore now be employed to
342 investigate long-term, decadal to centennial, controls on summer precipitation including the link between
343 precipitation and the AMO. Debate exists over the extent to which the AMO will change in the future beyond
344 natural fluctuations. Results from the IPCC AR5 report suggest that the AMO is unlikely to change its
345 behaviour in a warmer climate state (Christensen et al., 2013). However, comparisons have shown the
346 complexity in ensuring models adequately capture the characteristic of the AMO (Kavvada et al., 2013) whilst
347 evidence exists for an amplification of the AMO at the onset of industrial-era warming (Moore et al., 2017) and

348 so the potential for further modifications with increased SST.

349

350 On the basis of our composite $\delta^{18}\text{O}_{\text{diatom}}$ record from the south basin of Lake Baikal and the link to δ_{influx} and
351 $\delta^{18}\text{O}_p$ from 2011-1901 (Fig. 6a-c) we propose that $\delta^{18}\text{O}_{\text{diatom}}$ can be used to constrain annual precipitation and,
352 given the seasonal distribution of precipitation, the summer position of the Asiatic polar front and associated jet
353 system (Fig. 5b). This interpretation of $\delta^{18}\text{O}_{\text{diatom}}$ does not contradict previous records from Lake Baikal which
354 related changes in $\delta^{18}\text{O}_{\text{diatom}}$ to the balance of north and south basin river inputs in Lake Baikal and so the wider
355 hydroclimate of the region (Mackay et al., 2008, 2011, 2013). Instead, the relationship observed here now
356 permits an enhanced understanding of the palaeoclimatology of the region by disentangling the dominant
357 environmental controls on $\delta^{18}\text{O}_{\text{diatom}}$, precipitation and lake water temperature, allowing the quantification of
358 past changes in Central Asia precipitation.

359

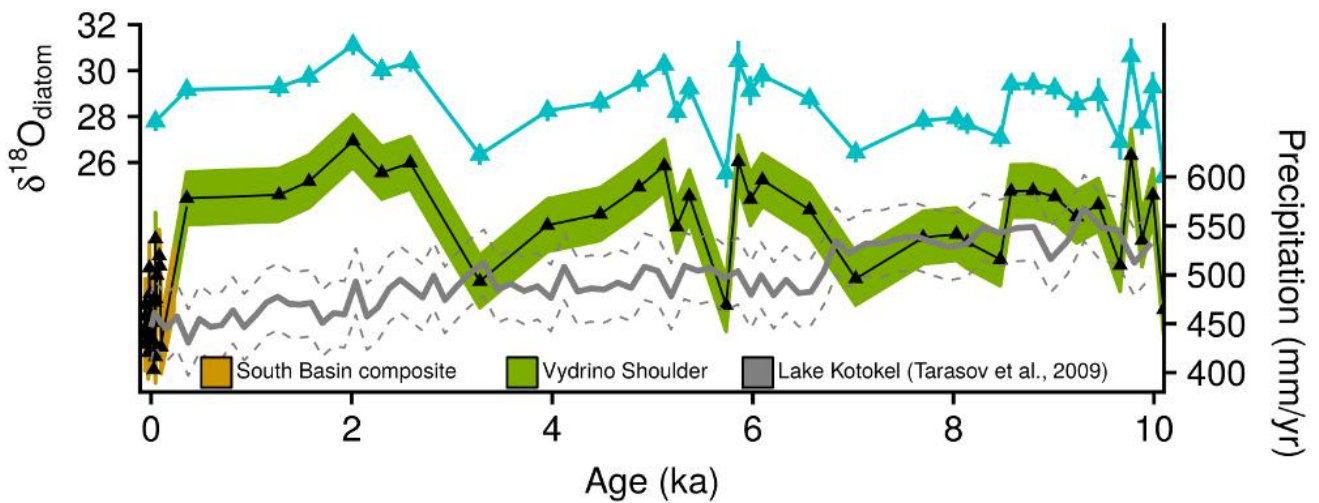
360 **4.2 Holocene reconstruction of Central Asian precipitation**

361 Precipitation data from Irkutsk is not available prior to 1891. Using the relationship between $\delta^{18}\text{O}_{\text{diatom}}$ and
362 precipitation from c. 2010-1900 (Fig. 6c) we quantify decadal changes in annual precipitation for Central Asia
363 from our composite south basin $\delta^{18}\text{O}_{\text{diatom}}$ record, which extends back to c. 1850 AD (Fig. 6d). Results show that
364 the degree of variability in 21st and 20th century precipitation also prevailed through the late 19th century (426-
365 519 mm/yr) with significantly lower levels of precipitation in c. 1850 relative to 1860-1890. Within the
366 constraints of this low-resolution record and the regression standard error of 26.9 mm/yr, the results suggest
367 that decadal annual precipitation in Central Asia has not notably changed in response to increased
368 global/regional air temperature over the last c. 160 years (Fig. 6d). Observed reductions in Central Asian
369 precipitation and river flow over recent decades (Liu et al., 2013; Li et al., 2015; Frolova et al., 2017) may
370 therefore represent natural variability rather than an anthropogenic driven change.

371

372 Tree ring records from Mongolia currently provide regional hydroclimate data for the last 500 years (Pederson
373 et al., 2001; Davi et al., 2006, 2009, 2010). However, longer precipitation records are needed, particularly over
374 abrupt climate transitions and from geological analogues for the future to fully assess trends in Central Asian
375 precipitation and possible links to the North Atlantic region. To place the results of the composite south basin
376 core over the last c. 200 years within the context of natural variability, long-term changes in Central Asian

377 precipitation are reconstructed from a previously published $\delta^{18}\text{O}_{\text{diatom}}$ record from Vydrino Shoulder (51.588N,
 378 104.858E, Fig. 1) located off the southern shoreline of Lake Baikal (Mackay et al., 2011) (Fig. 7). From 0-10
 379 ka annual precipitation ranges from c. 420-770 mm/yr ($\bar{x} = 570$ mm/yr, $1\sigma = 65$ mm/yr) with precipitation for
 380 most of the interval higher than that recorded at Irkutsk during the 21st and 20th Century ($\bar{x} = 450$ mm/yr) (Fig.
 381 5a, 7). No decline in precipitation occurs through the neoglacial from c. 4.0-0.2 ka, but significant variability is
 382 apparent through the mid-Holocene warm interval from 5-9 ka ($\bar{x} = 558$ mm/yr, $1\sigma = 41$ mm/yr). As such, with
 383 levels of Holocene precipitation only comparable to the mean modern day conditions at 5.7 ka and 10.1-10.2 ka
 384 (Fig. 7), the results indicate the potential for further changes in precipitation as the region responds to a future
 385 climate state.



386 Figure 7: Holocene $\delta^{18}\text{O}_{\text{diatom}}$ from Vydrino Shoulder (51.588N, 104.858E, Fig. 1) located off the southern
 387 shoreline of Lake Baikal (Mackay et al., 2011) together with reconstructed precipitation at Vydrino Shoulder
 388 (green) and in the south basin composite record (brown) displayed in Figure 6d. One sample from the Vydrino
 389 Shoulder core (0.04 ka / 1907 AD) overlaps with the composite record in Figure 6. Shaded region shows range
 390 of reconstructed precipitation based on the standard error (26.9 mm/yr) of the regression model between
 391 $\delta^{18}\text{O}_{\text{diatom}}$ and Irkutsk precipitation (Fig. 6c). Also shown is the pollen inferred precipitation record from Lake
 392 Kotokel (solid grey line) (Tarasov et al., 2009) and the associated root mean square error of prediction (RMSE)
 393 of 34 mm/yr (Solovieva et al. 2005).

394
 395 Reconstructed values of Holocene precipitation at Vydrino Shoulder are broadly comparable to patterns of
 396 effective summer precipitation obtained from a low-resolution general circulation model for the region (Bush,
 397 2005). Existing quantitative reconstructions of precipitation for the region immediately around Lake Baikal

398 have been derived from pollen records from Lake Baikal itself and nearby Lake Kotokel (Fig. 1), both showing
399 similar trends to one another through the Holocene (Tarasov et al., 2007, 2009). However, whereas levels of
400 precipitation at Lake Kotokel (pollen) and Vydrino Shoulder ($\delta^{18}\text{O}_{\text{diatom}}$) are similar through the early Holocene,
401 after c. 7 ka pollen inferred precipitation decreases by c. 10% with no corresponding change in the $\delta^{18}\text{O}_{\text{diatom}}$
402 derived record (Fig. 7). This decline in pollen derived precipitation in/around Lake Baikal contrasts with
403 records from the northern Mongolian Plateau which, similar to the $\delta^{18}\text{O}_{\text{diatom}}$ reconstruction, shows high rates of
404 precipitation in both the early and late Holocene (Wang and Feng, 2013). Whilst records on the northern
405 Mongolian plateau show a degree of spatial variability, no long-term decline in precipitation is apparent from c.
406 7 ka (Wang and Feng, 2013). Given the size of Lake Baikal's catchment (540,000 km²) and with 83% of
407 riverine inflow originating from the Selenga River and its tributaries, which extend into Mongolia, or the Upper
408 Angara and Barguzin Rivers, which drain the region immediately to the east and north of Lake Baikal (Fig. 1),
409 we suggest that our $\delta^{18}\text{O}_{\text{diatom}}$ precipitation record from Lake Baikal reflects an amalgamated average of
410 conditions across the wider Central Asian region rather than localised site-specific changes in precipitation. As
411 such, whilst pollen records in and around Lake Baikal suggest reduced precipitation in the late Holocene
412 (Tarasov et al., 2007, 2009), the higher $\delta^{18}\text{O}_{\text{diatom}}$ reconstructed precipitation at Lake Baikal reflects the fact that
413 rates of precipitation in north Mongolia did not decline between the early/late Holocene period.

414

415 With a relationship established between $\delta^{18}\text{O}_{\text{diatom}}$ and Central Asian precipitation, records of precipitation from
416 Lake Baikal have the potential to aid the development of future forecasts for the region. Models in the Coupled
417 Model Intercomparison Project (CMIP5) are currently not able to confidently predict future changes in Central
418 Asian precipitation (Christensen et al., 2013), but together with regional models they indicate the potential for
419 decreases in precipitation for northern Mongolia and the Lake Baikal catchment, leading to associated
420 reductions in soil moisture and increased vulnerability to drought and fire (Sato et al., 2007; Törnqvist et al.,
421 2014). Data-model comparisons under the Paleoclimate Modelling Intercomparison Project (PMIP) highlight
422 the complexities in generating accurate simulation of precipitation for the mid-Holocene (Bartlein et al., 2010;
423 Braconnot et al., 2012). Whereas PMIP3 simulations suggest no notable change between 6 ka and pre-industrial
424 conditions, our results show that regional precipitation at 6 ka was c. 25% higher than modern day precipitation
425 (450 mm/yr) and c. 30% higher than the reconstructed precipitation of 430 mm/yr in pre-industrial conditions at
426 c. 1850 AD (Fig. 7). Consequently, integration of $\delta^{18}\text{O}_{\text{diatom}}$ precipitation data from Lake Baikal within ongoing

427 modelling efforts should aid future model validation for Central Asia.

428

429 **5 Conclusions**

430 There is uncertainty over the potential for future changes in Central Asian precipitation under a warmer climate
431 state, changes which have severe implications for the grassland-taiga ecotone and carbon cycling in the region.
432 By comparing records of $\delta^{18}\text{O}_{\text{diatom}}$ to local meteorological data for the last 100 years we demonstrate an
433 empirical relationship in Lake Baikal between $\delta^{18}\text{O}_{\text{diatom}}$ and Central Asian precipitation, providing an
434 opportunity to study the long-term variability of regional precipitation together with the position of the Asiatic
435 polar front and link to the AMO. Accordingly, records from Lake Baikal are able to aid future climate
436 predictions by investigating geological intervals that might represent an analogue of a future climate state and
437 through data-model comparisons with the PMIP community. In contrast to current models, results from
438 $\delta^{18}\text{O}_{\text{diatom}}$ show that precipitation has varied significantly over the last 10 ka, indicating the region's potential
439 sensitivity to a perturbation in the climate system. With levels of precipitation over the past c. 160 years either
440 at or close to their lowest levels of the last 10 ka, the potential exists for further reductions to significantly
441 impact water availability and societies across Central Asia.

442

443 **References**

- 444 Afanasyev, A.N., 1976. The Water Resources and Water Balance of Lake Baikal Basin. Nauka Publishers, Novosibirsk.
445 (in Russian).
- 446 Appleby, P.G., Oldfield, F., 1978. The calculation of ^{210}Pb dates assuming a constant rate of supply of unsupported ^{210}Pb to
447 the sediment. *Catena* 5, 1-8.
- 448 Appleby, P.G., Nolan, P.J., Gifford, D.W., Godfrey, M.J., Oldfield, F., Anderson, N.J., Battarbee, R.W., 1986. ^{210}Pb dating
449 by low background gamma counting. *Hydrobiologia* 141, 21-27.
- 450 Appleby, P.G., Richardson, N., Nolan, P.J., 1992. Self-absorption corrections for well-type germanium detectors. *Nucl.*
451 *Instrum, Meth, B.* 71, 228-233.
- 452 Bartington Instruments 1995. Operation Manual MS2. Bartington Instruments, Oxford,
453 <http://www.bartington.com/Literaturepdf/Operation%20Manuals/om0408%20MS2.pdf>.
- 454 Bartlein, P.J., Harrison, S.P., Brewer, S., Connor, S., Davis, B.A.S., Gajewski, K., Guiot, J., Harrison-Prentice, T.I.,
455 Henderson, A., Peyron, O., Prentice, I.C., Scholze, M., Seppä, H., Shuman, B., Sugita S., Thompson, R.S., Viau, A.E.,
456 Williams, J., Wu, H., 2010. Pollen-based continental climate reconstructions at 6 and 21 ka: a global synthesis. *Clim.*
457 *Dyn.* 3-4, 775-802.
- 458 Braconnot, P., Harrison, S.P., Kageyama, M., Bartlein, P.J., Masson-Delmotte, V., Abe-Ouchi, A., Otto-Bliesner, B.,
459 Zhao, Y., 2012 Evaluation of climate models using palaeoclimatic data. *Nat. Clim. Change* 2, 417-424.
- 460 Brewer, T., Leng, M., Mackay, A.W., Lamb, A., Tyler, J., Marsh, N., 2008. Unravelling contamination signals in biogenic
461 silica oxygen isotope composition: the role of major and trace element geochemistry. *J Quaternary Sci.* 23, 365-374.
- 462 Bush, A.B.G., 2005. $\text{CO}_2/\text{H}_2\text{O}$ and orbitally driven climate variability over central Asia through the Holocene. *Quatern.*
463 *Int.* 136, 15-23.
- 464 Chaplignin, B., Leng, M.J., Webb, E., Alexandre, A., Dodd, J.P., Ijiri, A., Lücke, A., Shemesh, A., Abelmann, A.,

- 465 Herzschuh, U., Longstaffe, F.J., Meyer, H., Moschen, R., Okazaki, Y., Rees, N., Sharp, Z.D., Sloane, H.J., Sonzogni,
466 C., Swann, G.E.A., Sylvestre, F., Tyler, J.T., Yam, R., 2011. Inter-laboratory comparison of oxygen isotopes from
467 biogenic silica. *Geochim. Cosmochim. Ac.* 75, 7242-7256.
- 468 Chen, S.-J., Kuo, Y.-H., Zhang, P.-Z., Bai, Q.-F., 1991. Synoptic climatology of cyclogenesis over East Asia. *Mon. Weather*
469 *Rev.* 119, 1407-1418.
- 470 Christensen, J.H., Krishna Kumar, K., Aldrian, E., An, S.-I., Cavalcanti, I.F.A., de Castro, M., Dong, W., Goswami, P.,
471 Hall, A., Kanyanga, J.K., Kitoh, A., Kossin, J., Lau, N.-C., Renwick, J., Stephenson, D.B., Xie, S.-P., Zhou, T., 2013.
472 Climate Phenomena and their Relevance for Future Regional Climate Change. In: *Climate Change 2013: The Physical*
473 *Science Basis. Contribution of Working Group I to the Fifth Assessment Report of the Intergovernmental Panel on*
474 *Climate Change* [Stocker, T.F., Qin, D., Plattner, G.-K., Tignor, M., Allen, S.K., Boschung, J., Nauels, A., Xia, Y., Bex,
475 V. Midgley, P.M. (eds.)]. Cambridge University Press, Cambridge, United Kingdom and New York, NY, USA.
- 476 Craine, J.M., Nippert, J.B., Elmore, A.J., Skibbe, A.M., Hutchinson, S.L., Brunzell, N.A., 2012, Timing of climate
477 variability and grassland productivity. *109, P. Natl. Acad. Sci, USA.* 3401-3405.
- 478 Crowther, T.W., Todd-Brown, K.E.O., Rowe, C.W., Wieder, W.R., Carey, J. C., Machmuller, M.B., Snoek, B.L., Fang, S.,
479 Zhou, G., Allison, S.D., Blair, J.M., Bridgham, S.D., Burton, A.J., Carrillo, Y., Reich, P.B., Clark, J.S., Classen, A.T.,
480 Dijkstra, F.A., Elberling, B., Emmett, B.A., Estiarte, M., Frey, S.D., Guo, J., Harte, J., Jiang, L., Johnson, B.R., Kröel-
481 Dulay, G., Larsen, K.S., Laudon, H., Lavallee, J.M., Luo, Y., Lupascu, M., Ma, L.N., Marhan, S., Michelsen, A.,
482 Mohan, J., Niu, S., Pendall, E., Peñuelas, J., Pfeifer-Meister, L., Poll, C., Reinsch, S., Reynolds, L.L., Schmidt, I.K.,
483 Sistla, S., Sokol, N.W., Templer, P.H., Treseder, K.K., Welker, J.M., Bradford, M.A., 2016. Quantifying global soil
484 carbon losses in response to warming. *Nature* 540, 104-108.
- 485 Davi, N.K., Jacoby, G.C., Curtis, A.E., Nachin, B., 2006. Extension of drought records for central Asia using tree rings:
486 West central Mongolia. *J. Clim.*, 19, 288-299..
- 487 Davi, N., Jacoby, G., D'Arrigo, R., Baatarbileg, N., Li, J., Curtis, A., 2009. A tree-ring based drought index reconstruction
488 for far western Mongolia: 1565–2004. *Int. J. Climatol.* 29, 1508-1514.
- 489 Davi, N., Jacoby, G., Fang, K., Li, J., D'Arrigo, R., Baatarbileg, N., Robinson, D., 2010. Reconstructing drought
490 variability for Mongolia based on a large-scale tree ring network: 1520-1993. *J. Geophys. Res.* 115, D22103.
- 491 Endo, N., Kadota, T., Matsumoto, J., Ailikun, B., Yasunari, T., 2006. Climatology and Trends in Summer Precipitation
492 Characteristics in Mongolia for the Period 1960–98. *J. Meteorol. Soc. Jpn.* 84, 543-551.
- 493 Frolova, N.L., Belyakova, P.A., Grigoriev, V.Y., Sazonov, A.A., Zotov, L.V., Jarsjö, J., 2017. Runoff fluctuations in the
494 Selenga River Basin. *Reg. Environ. Change.* doi:10.1007/s10113-017-1199-0.
- 495 Forkel, M., Thonicke, K., Beer, C., Cramer, W., Bartalev, S., Schmullius, C., 2012. Extreme fire events are related to
496 previous-year surface moisture conditions in permafrost-underlain larch forests of Siberia. *Environ. Res. Lett.* 7,
497 044021.
- 498 Hansen, M.C., Potapov, P.V., Moore, R., Hancher, M., Turubanova, S.A., Tyukavina, A., Thau, D., Stehman, S.V.,
499 Goetz, S.J., Loveland, T.R., Kommareddy, A., Egorov, A., Chini, L., Justice, C.O., Townshend, J.R.G., 2013. High-
500 resolution global maps of 21st-century forest cover change. *Science* 342, 850-853.
- 501 Haywood, A.M., Dowsett, H.J., Dolan, A.M., 2016. Integrating geological archives and climate models for the mid-
502 Pliocene warm period. *Nat. Commun.* 7, 10646.
- 503 Hijjoka, Y., Lin, E., Pereira, J.J., Corlett, R.T., Cui, X., Insarov, G.E., Lasco, R.D., Lindgren, E., Surjan, A., 2014. Asia,
504 in: Barros, V.R., Field, C.B., Dokken, D.J., Mastrandrea, M.D., Mach, K.J., Bilir, T.E., Chatterjee, M., Ebi, K.L.,
505 Estrada, Y.O., Genova, R.C., Girma, B., Kissel, E.S., Levy, A.N., MacCracken, S., Mastrandrea, P.R., White, L.L.
506 (Eds.), *Climate Change 2014: Impacts, Adaptation, and Vulnerability. Part B: Regional Aspects. Contribution of*
507 *Working Group II to the Fifth Assessment Report of the Intergovernmental Panel on Climate Change.* Cambridge
508 University Press, Cambridge, United Kingdom and New York, NY, USA, pp. 1327-1370.
- 509 Hohmann R., Kipfer R., Peeters F., Piepke G., Imboden D.M., Shimaraev M.N., 1997. Deep-water renewal in Lake Baikal.
510 *Limnol. Oceanogr.* 42, 841-855.
- 511 IPCC, 2012. Managing the Risks of Extreme Events and Disasters to Advance Climate Change Adaptation. A Special
512 Report of Working Groups I and II of the Intergovernmental Panel on Climate Change, in: Field, C.B., Barros, V.,
513 Stocker, T.F., Qin, D., Dokken, D.J., Ebi, K.L., Mastrandrea, M.D., Mach, K.J., Plattner, G.-K., Allen, S.K., Tignor, M.,
514 Midgley, P.M. (Eds.), Cambridge University Press, Cambridge, UK, and New York, NY, USA, 582 pp.
- 515 Iwao, K., Ttakahashi, M., 2006. Interannual change in summertime precipitation over northeast Asia. *Geophys. Res. Lett.*
516 33, L16703.
- 517 Iwao, K., Ttakahashi, M., 2008. A Precipitation seesaw mode between Northeast Asia and Siberia in Summer caused by
518 Rossby waves over the Eurasian continent. *J. Clim.* 21, 2401-2419.

- 519 Karthe, D., Chalov, S., Borchardt, D., 2015. Water resources and their management in central Asia in the early twenty first
520 century: status, challenges and future prospects. *Environ. Earth. Sci.* 73, 487-499.
- 521 Kavvada, A., Ruiz-Barradas, A., Nigam, S., 2013. AMO's structure and climate footprint in observations and IPCC AR5
522 climate simulations. *Clim. Dyn.* 41, 1345-1364.
- 523 Kipfer R., AeschbachHertig W., Hofer M., Hohmann R., Imboden D.M., Baur H., Golubev V., Klerkx J., 1996.
524 Bottomwater formation due to hydrothermal activity in Frolikha Bay, Lake Baikal, eastern Siberia. *Geochim.*
525 *Cosmochim. Acta.* 60, 961-971.
- 526 Leng, M.J., Barker, P., 2006. A review of the oxygen isotope composition of lacustrine diatom silica for palaeoclimate
527 reconstruction. *Earth Sci. Rev.* 75, 5-27.
- 528 Leng, M.J., Sloane, H.J., 2008. Combined oxygen and silicon isotope analysis of biogenic silica. *Journal of Quaternary*
529 *Science* 23, 313-319.
- 530 Li, C., Zhang, C., Luo, G., Chen, X., Maisupova, B., Madaminov, A.A., Han, Q., Djenbaev, B.M., 2015. Carbon stock and
531 its responses to climate change in Central Asia. *Glob. Change. Biol.* 21, 1951-1967.
- 532 Liu, Y.Y., Evans, J.P., McCabe, M.F., de Jeu, R.A.M., van Dijk, A.I.J.M., Dolman, A.J., Saizen, I., 2013. Changing
533 Climate and Overgrazing Are Decimating Mongolian Steppes. *PLOS One* 8, e57599.
- 534 Lu, Y., Zhuang, Q., Zhou, G., Sirin, A., Melillo, J., Kicklighter, D., 2009. Possible decline of the carbon sink in the
535 Mongolian Plateau during the 21st century. *Environ. Res. Lett.* 4, 045023.
- 536 Lydolph, P.E., 1977. Eastern Siberia. In: *Climates of the Soviet Union. World Survey of Climatology*, vol. 7. Elsevier, pp.
537 91-115.
- 538 Mackay, A.W., Karabanov, E., Khursevich, G., Leng, M., Morley, D.W., Panizzo, V.N., Sloane, H.J., Williams, D., 2008.
539 Reconstructing hydrological variability in Lake Baikal during MIS 11: an application of oxygen isotope analysis of
540 diatom silica. *J Quaternary Sci.*, 23, 365-374.
- 541 Mackay, A.W., Swann, G.E.A., Brewer, T., Leng, M.J., Morley, D.W., Piotrowska, N., Rioual, P., White, D., 2011. A
542 reassessment of late glacial-Holocene diatom oxygen isotope records from Lake Baikal using a mass balance approach.
543 *J Quaternary Sci.* 26, 627-634
- 544 Mackay, A.W., Swann, G.E.A., Fagel, N., Fietz, S., Leng, M.J., Morley, D., Rioual, P., Tarasov, P. 2013., Hydrological
545 instability during the Last Interglacial in central Asia: a new diatom oxygen isotope record from Lake Baikal.
546 *Quaternary Sci. Rev.* 66, 45-54.
- 547 Mackay, A.W., Seddon, A.W.R., Leng, M.J., Heumann, G., Morley, D.W., Piotrowska, N., Rioual, P., Roberts, S., Swann,
548 G.E.A., 2017. Holocene carbon dynamics at the forest - steppe ecotone of southern Siberia. *Glob. Change Biol.* 23,
549 1942-1960.
- 550 Moore, G.W.K., Halfar, J., Majeed, H., Adey, W., Kronz, A., 2017, Amplification of the Atlantic Multidecadal Oscillation
551 associated with the onset of the industrial-era warming. *Sci Rep-UK*, 7:40861.
- 552 Moore, M.V., Hampton, S.E., Izmet'eva, L.R., Silow, E.A., Peshkova, E.V., Pavlov, B.K., 2009. Climate Change and the
553 World's "Sacred Sea"-Lake Baikal, Siberia. *BioScience* 49, 405-417.
- 554 Morley, D.W., Leng, M.J., Mackay, A.W., Sloane, H.J., 2005. Late Glacial and Holocene atmospheric circulation change
555 in the Lake Baikal region documented by oxygen isotopes from diatom biogenic silica. *Global Planet. Change* 46, 221-
556 233
- 557 Pederson, N., Jacoby, G., D'Arrigo, R., Cook, E., Buckley, B., Dugarjav, C., Mijiddorj, R., 2001. Hydrometeorological
558 reconstructions for north-eastern Mongolia derived from tree rings: AD 1651-1995, *J. Clim.* 14, 872-881.
- 559 Popovskaya, G.I., 2000. Ecological monitoring of phytoplankton in Lake Baikal. *Aquatic Ecosystem Health and*
560 *Management* 3, 215-225.
- 561 Randerson, J.T., Liu, H., Flanner,, M.G., Chambers, S.D., Jin, Y., Hess, P.G., Pfister,, G., Mack, M.C., Treseder,, K.K.,
562 Welp, L.R., Chapin, F.S., Harden,, J.W., Goulden,, M.L., Lyons,, E., Neff, J.C., Schuur,, E.A.G., Zender, C.S., 2006.
563 The Impact of Boreal Forest Fire on Climate Warming. *Science* 314, 1130-1132.
- 564 Ravens, T.M., Kocsis, O., Wüest, A., Granin, N., 2000. Small-scale turbulence and vertical mixing in Lake Baikal.
565 *Limnol. Oceanogr.* 45, 159-173.
- 566 Romanovsky, V.E., Drozdov, D.S., Oberman, N.G., Malkova, G.V., Kholodov, A.L., Marchenko, S.S., Moskalenko, N.G.,
567 Sergeev, D.O., Ukraintseva, N.G., Abramov, A.A., Gilichinsky, D.A., Vasiliev, A.A., 2010., Thermal state of
568 permafrost in Russia. *Permafrost Periglac.* 21, 136-155.
- 569 Sato, T., Kimura, F., Kitoh, A., 2007. Projection of global warming onto regional precipitation over Mongolia using a
570 regional climate model. *J. Hydrol.* 333, 144-154.

- 571 Schuur, E.A.G., McGuire, A.D., Schädel, C., Grosse, G., Harden, J.W., Hayes, D.J., Hugelius, G., Koven, C.D., Kuhry, P.,
572 Lawrence, D.M., Lawrence, S.M., Olefeldt, D., Romanovsky, V.E., Schaefer, K., Turetsky, M.R., Treat, C.C., Vonk,
573 J.E., 2015. Climate change and the permafrost carbon feedback. *Nature* 520, 171-179.
- 574 Seal, R.R., Shanks, W.C., 1998. Oxygen and hydrogen isotope systematics of Lake Baikal, Siberia: implications for
575 palaeoclimate studies. *Limnol. Oceanogr.* 43, 1251-1261.
- 576 Selvam, B.P., Lapierre, J-F., Guillemette, F., Voigt, C., Lamprecht, R.E., Biasi, C., Christensen, T.R., Martikainen, P.J.,
577 Berggren, M., 2017. Degradation potentials of dissolved organic carbon (DOC) from thawed permafrost peat. *Sci Rep-
578 UK* 7, 45811.
- 579 Settele, J., Scholes, R., Betts, R., Bunn, S., Leadley, P., Nepstad, D., Overpeck, J.T., Taboada, M.A., 2014, Terrestrial and
580 inland water systems, in Field, C.B., Barros, V.R., Dokken, D.J., Mach, K.J., Mastrandrea, M.D., Bilir, T.E., Chatterjee,
581 M., Ebi K.L., Estrada, Y.O., Genova, R.C., Girma, B., Kissel, E.S., Levy, A.N., MacCracken, S., Mastrandrea, P.R.,
582 White, L.L. (Eds.), *Climate Change 2014: Impacts, Adaptation, and Vulnerability. Part A: Global and Sectoral Aspects.*
583 *Contribution of Working Group II to the Fifth Assessment Report of the Intergovernmental Panel on Climate Change.*
584 Cambridge University Press, Cambridge, United Kingdom and New York, NY, USA, pp. 271-359.
- 585 Shahgedanova, M., 2002. Climate at present and in the historical past. In: Shahgedanova, M. (Ed.), *The Physical
586 Geography of Northern Eurasia.* OUP, Oxford, pp. 70-102.
- 587 Sharkuu N., 1998. Trends in permafrost development in the Selenge River basin, Mongolia. *Collection Nordicana*, 55,
588 979-985.
- 589 Shimaraev M.N., Granin N.G., 1991. Temperature stratification and the mechanisms of convection in Lake Baikal. *Dokl.
590 Akad. Nauk.* 321, 381-385.
- 591 Shimaraev M.N., Domysheva V.M., 2004. Climate and long-term silica dynamics in Lake Baikal. *Russ. Geol. Geophys.*
592 45, 310-316.
- 593 Shimaraev M.N., Granin N.G., Zhdanov A.A., 1993. Deep ventilation of Lake Baikal waters due to spring thermal bars.
594 *Limnol. Oceanogr.* 38, 1068-1072.
- 595 Shimaraev, M.N., Verbolov, V.I., Granin, N.G., Sherstyankin, P.P., 1994. Physical Limnology of Lake Baikal. A review.
596 In: Shimaraev, M.N., Okuda, S. (Eds.), *BICER Publishers, Irkutsk.* 81 pp.
- 597 Shimaraev, M.N., Troitskaya, E.S., Blinov, V.V., Ivanov, V.G., Gnatovskii, R.Yu., 2012. Upwellings in Lake Baikal.
598 *Dokl. Earth Sc.* 442, 272-276.
- 599 Solovieva, N, Tarasov P.E., MacDonald, G., 2005. Quantitative reconstruction of Holocene climate from the Chuna Lake
600 pollen record, Kola Peninsula, northwest Russia. *Holocene* 15, 141-148.
- 601 Sturm M., Vologina E.G., Vorob'eva S.S., 2016. Holocene and Late Glacial sedimentation near steep slopes in southern
602 Lake Baikal. *J. Limnology.* 75, 24-35.
- 603 Sugita, M., Yoshizawa, S., Byambakhuu, I., 2015, Limiting factors for nomadic pastoralism in Mongolian steppe: a
604 hydrologic perspective. *J. Hydrol.* 524, 455-467.
- 605 Sun, C., Li, J., Zhao, S., 2015. Remote influence of Atlantic multidecadal variability on Siberian warm season
606 precipitation. *Sci. Rep-UK.* 5, 16853.
- 607 Swann, G.E.A., Pike, J., Snelling, A.M., Leng, M.J., Williams, M.C., 2013. Seasonally resolved diatom $\delta^{18}\text{O}$ records from
608 the west Antarctic Peninsula over the last deglaciation. *Earth Planet. Sci. Lett.* 364, 12-23.
- 609 Tarasov, P., Bezrukova, E., Karabanov, E., Nakagawa, T., Wagner, M., Kulagina, N., Letunova, P., Abzaeva, A.,
610 Granoszewski, W., Riedel, F., 2007. Vegetation and climate dynamics during the Holocene and Eemian interglacials
611 derived from Lake Baikal pollen records. *Palaeogeogr. Palaeocl.* 252, 440-457.
- 612 Tarasov, P.E., Bezrukova, E.V., Krivonogov, S.K., 2009. Late Glacial and Holocene changes in vegetation cover and
613 climate in southern Siberia derived from a 15 kyr long pollen record from Lake Kotokel. *Clim. Past.* 5, 285-295.
- 614 Tautenhahn, S.T., Lichstein, J.W., Jung, M., Kattge, J., Bohlman, S.A., Heilmeyer, H., Prokushkin, A., Kahl, A., Wirth, C.,
615 2016. Dispersal limitation drives successional pathways in Central Siberian forests under current and intensified fire
616 regimes. *Glob. Change Biol.* 22, 2178-2197.
- 617 Tchebakova, N.M., Parfenova, E., Soja, A.J., 2009. The effects of climate, permafrost and fire on vegetation change in
618 Siberia in a changing climate. *Environ. Res. Lett.* 4 045013.
- 619 Tchebakova, N.M., Parfenova, E.I., Korets, M.A., Conard, S.G., 2016. Potential change in forest types and stand heights in
620 central Siberia in a warming climate. *Environ. Res. Lett.* 11, 035016.
- 621 Törnqvist, R., Jarsjö, J., Pietroni, J., Bring, A., Rogberg, P., Asokan, S.M., Destouni, G., 2014. Evolution of the hydro-
622 climate system in the Lake Baikal basin. *J. Hydrol.* 519, 1953-1962.

- 623 Troitskaya, E., Blinov, V., Ivanov, V., Zhdanov, A., Gnatovsky, R., Sutyryna, E., Shimaraev, M., 2015. Cyclonic
624 circulation and upwelling in Lake Baikal. *Aquat. Sci.* 77, 171-182.
- 625 Tsimitri, C., Rockel, B., Wüest, A., Budnev, N.M., Sturm, M., Schmid, M., 2015. Drivers of deep-water renewal events
626 observed over 13 years in the South Basin of Lake Baikal. *J. Geophys. Res. Oceans*, 120, 1508-1526.
- 627 Vologina, E.G., Kashik, S.A., Sturm, M., Vorob'eva, S.S., Lomonosova, T.K., Kalashnikova, I.A., Khramtsova, T.I.,
628 Toshchakov, S.Yu., 2007. Results of research into Holocene sediments of the South and Central basins of Lake Baikal
629 (BDP-97 and short cores). *Russ. Geol. Geophys.* 48, 312-323.
- 630 Weiss, R.F., Carmak, E.C., Koropalov, V.M., 1991. Deep-water renewal and biological production in Lake Baikal. *Nature*
631 349, 665-669.
- 632 Wang, W., Feng, Z., 2013. Holocene moisture evolution across the Mongolian Plateau and its surrounding areas: A
633 synthesis of climatic records. *Earth-Sci. Rev.* 122, 38-57.
- 634 Wu, X, Liu, H, Guo, D, Anenkhonov, O.A., Badmaeva, N.K., Sanddanov, D.V., 2012. Growth Decline Linked to
635 Warming-Induced Water Limitation in Hemi-Boreal Forests. *PLoS ONE* 7, e42619. doi:10.1371/journal.pone.0042619.
- 636 Zhao, L., Wu, Q., Marchenko, S.S., Sharkuu, N., 2010. Thermal state of permafrost and active layer in central Asia during
637 the International Polar Year. *Permafrost Periglac.* 21, 198-207.

638

639 **Acknowledgements**

640 This work was supported by Natural Environment Research Council grants NE/J00829X/1, NE/J010227/1, and
641 NE/J007765/1). The authors are indebted to the assistance of Nikolaj M. Budnev (Irkutsk State University), the
642 captain and crew of the Geolog research boat together with Dmitry Gladkochub (IEC) in facilitating and
643 organizing all Russian fieldwork. A final thanks is owed to Neil Rose and Handong Yang who carried out the
644 ²¹⁰Pb dating at the UCL Environmental Radiometric Facility.

645

646 **Supplementary Information**

647 Supplementary Table 1: Diatom oxygen isotope ($\delta^{18}\text{O}_{\text{diatom}}$) and reconstructed precipitation for south basin
648 sediment cores BAIK13-1C, BAIK13-4F and BAIK13-7A used in the composite $\delta^{18}\text{O}_{\text{diatom}}$ record.

649

650 Supplementary Table 2: Holocene $\delta^{18}\text{O}_{\text{diatom}}$ from Vydrino Shoulder (Lake Baikal) (Mackay et al., 2011) and
651 reconstructed precipitation.